

## ACKNOWLEDGMENTS

This work was supported in part by U.S. Public Health Service Grant CA-54891. We appreciate the assistance of Anil Maddukuri and Dr. Eun-Sook Cho in carrying out this work.

## REFERENCES

- Langmuir VK, Fowler JF, Knox SJ, Wessels BW, Sutherland RM, Wong JYC. Radiobiology of radiolabeled antibody therapy as applied to tumor dosimetry. *Med Phys* 1993;20:601-610.
- Fowler JF. Radiobiological aspects of low dose rates in radioimmunotherapy. *Int J Radiat Oncol Biol Phys* 1990;18:1261-1269.
- Rao DV, Howell RW. Time dose fractionation in radioimmunotherapy: implications for selecting radionuclides. *J Nucl Med* 1993;34:1801-1810.
- Howell RW, Goddu SM, Rao DV. Application of the linear-quadratic model to radioimmunotherapy: further support for the advantage of longer-lived radionuclides. *J Nucl Med* 1994;35:1861-1869.
- Bigler RE, Zanzonico PB, Leonard R, et al. Bone marrow dosimetry for monoclonal antibody therapy. In: Watson EE, Shlafke-Stelson AT, eds. *Proceedings of the Fourth International Radiopharmaceutical Dosimetry Symposium*. Springfield, VA: National Technical Information Service, U.S. Department of Commerce; 1986:535-544.
- Eary JF, Badger CC, Appelbaum FR, Durack L, Brown P. Determination of uptake and clearance of a nonspecific <sup>131</sup>I-labeled antibody in bone marrow [Abstract]. *J Nucl Med* 1989;30:826.
- Sgouros G. Bone marrow dosimetry for radioimmunotherapy: theoretical considerations. *J Nucl Med* 1993;34:689-694.
- Siegel JA, Pawlyk DA, Lee RE, et al. Tumor, red marrow, and organ dosimetry for <sup>131</sup>I-labeled anti-carcinoembryonic antigen monoclonal antibody. *Cancer Res* 1990;50:(suppl):1039s-1042s.
- Popp S, Cremer T. Development of a biological dosimeter for translocation scoring based on two-color fluorescence in situ hybridization of chromosome subsets. *J Radiat Res* 1992;33:(suppl):61-70.
- Lenarczyk M, Slowikowska MG. The micronucleus assay using peripheral blood reticulocytes from x-ray exposed mice. *Mutation Res* 1995;335:229-234.
- Metcalf D. *Hemopoietic colonies: in vitro cloning of normal and leukemic cells*. Berlin: Springer-Verlag; 1977.
- Testa NG. Clonal assays for haemopoietic and lymphoid cells in vitro. In: Potten CS, Hendry JH, eds. *Cell clones: manual of mammalian cell techniques*. Edinburgh, Scotland: Churchill-Livingstone; 1985:27-43.
- Takiue M, Natake T, Fujii H, Aburai T. Accuracy of Cerenkov measurements using a liquid scintillation spectrometer. *Appl Radiat Isot* 1996;47:123-126.
- Coursey BM, Calhoun JM, Cessna JT. Radioassays of yttrium-90 used in nuclear medicine. *Nucl Med Biol* 1993;20:693-699.
- Browne E, Firestone RB. *Table of radioactive isotopes*. New York: Wiley; 1986.
- Howell RW, Goddu SM, Rao DV. Design and performance of an experimental <sup>137</sup>Cs irradiator to simulate internal radionuclide dose rate patterns. *J Nucl Med* 1997;38:727-730.
- Hui TE, Fisher DR, Kuhn JA, et al. A mouse model for calculating cross-organ beta doses from yttrium-90-labeled immunoconjugates. *Cancer* 1994;73:(suppl):951-957.
- Barendsen GW. Dose fractionation, dose rate and iso-effect relationships for normal tissue responses. *Int J Radiat Oncol Biol Phys* 1982;8:1981-1997.
- Ramsden EN. A review of the experimental work on radio-yttrium comprising the tissue distribution, the mechanism of deposition in bone and the state in blood. *Int J Radiat Biol* 1961;3:399-410.
- Wu C-T, Lajtha LG. Haemopoietic stem-cell kinetics during continuous irradiation. *Int J Radiat Biol* 1975;27:41-50.
- International Commission on Radiological Protection. *RBE for deterministic effects* (Publication no. 58). Oxford, England: Pergamon Press 1989.
- International Commission on Radiological Protection. *1990 recommendations* (Publication no. 60). Oxford, England: Pergamon Press; 1991.
- Neben S, Anklesaria P, Greenberger J, Mauch P. Quantitation of murine hematopoietic stem cells in vitro by limiting dilution analysis of cobblestone area formation on a clonal stromal cell line. *Exp hematol* 1993;21:438-443.
- Ploemacher RE, van der Sluijs JP, Voerman JSA, Brons NHC. An in vitro limiting-dilution assay of long-term repopulating hematopoietic stem cells in the mouse. *Blood* 1989;74:2755-2763.

# An Alternative Method to Normalize Clinical FDG Studies

Anders Sandell, Tomas Ohlsson, Kjell Erlandsson and Sven-Erik Strand  
*Department of Radiation Physics, University Hospital, Lund, Sweden*

An alternative method of determining the integrated input function, necessary in the quantitative [<sup>18</sup>F]fluorodeoxyglucose (FDG) autoradiographic model, has been developed. Using erythrocytes as reference tissue, researchers require only one blood sample after injection of FDG to obtain the integrated input function. **Methods:** The amount of FDG-6-PO<sub>4</sub> in the erythrocytes is proportional to their exposure to FDG, that is, the integrated input function. Free FDG is removed by washing the erythrocytes twice. Inter- and intraindividual differences of the metabolic rate of erythrocytes are corrected for by an in vitro incubation with a known amount of FDG. **Results:** Validation of the proposed method was done by correlating the integrated input function, based on the glucose metabolism of the erythrocytes, to the integrated input function obtained by multiple venous blood samples. The new method provides the integrated input function with an accuracy better than ±8%. **Conclusion:** By using erythrocytes as a reference tissue, researchers can determine the integrated input function in the quantitative FDG autoradiographic model with an accuracy sufficient for clinical PET studies. The simplicity of the method also makes it suitable for FDG studies on small children. With two samples, the method can also be used for a simplified graphical Patlak analysis.

**Key Words:** erythrocytes; fluorine-18-fluorodeoxyglucose; integrated input function; normalization

**J Nucl Med** 1998; 39:552-555

The problem of finding a simplified way of normalizing FDG-PET measurements has been addressed by different groups. The orthodox straightforward way is to use arterial blood samples to calculate the integrated FDG-input function. This, however, requires numerous samples and is a slightly traumatic experience for the patient. Phelps et al. (1) showed that the arterial samples could be replaced by venous samples. The blood activity in the aorta, measured with the PET scanner, has been used for the input function when the aorta is included in the field of view (2). Takikawa et al. (3) also developed a method using a population-based arterial blood curve.

A highly simplified method adopted by several groups is to only use the injected activity divided by body weight (SUV<sub>bw</sub>) or body surface area (SUV<sub>bsa</sub>). There are specific problems when using these indices (4,5), even after correcting for blood glucose concentration. A further discussion on these indices can be found in an editorial by Fischman AJ, et al. (6). When a reference tissue is used to normalize an FDG measurement, cerebellum seems to be the best choice (7). This, however, often requires an additional PET scan.

This article describes a new method based on the glucose metabolism of the erythrocytes, requiring only one blood sample taken in the middle of the PET scan to provide the integrated input function.

## THEORY

Definitions of the symbols used in this article are listed in Table 1.

Consider an equation describing the metabolic rate (MR) of

Received Jul. 29, 1996; revision accepted May 6, 1997.

For correspondence or reprints contact: Anders Sandell, MSC, Department of Radiation Physics, University Hospital, S-221 85 Lund, Sweden.

glucose for some noninsulin dependent tissue, e.g. a tumor ( $\delta$ ), with  $k_4^*$  being omitted:

$$MR = \frac{C_{gl}}{LC} \frac{C_1^*(T) - \frac{k_1^* k_2^*}{k_2^* + k_3^*} \int_0^T e^{-(k_2^* + k_3^*)(T-t)} C_p^*(t) dt}{\int_0^T C_p^*(t) dt}. \quad \text{Eq. 1}$$

In brain studies, the second term in the numerator is calculated using standard transport coefficients. This term represents the radioactivity of nonmetabolized FDG, measured with the scanner, which for nonbrain tumors is set to zero at reasonably late times,  $\sim 45$  min postinjection. Setting this term to zero corresponds to a situation where a Gjedde-Patlak plot is based on two points, one at  $\sim 45$  min postinjection and the other at the origin. This, of course, gives an overestimation of the metabolic rate, probably by 10%–20%. With  $LC = 1$ , the following equation, also used by Rhodes et al. (9), is obtained:

$$MR = \frac{C_{gl} \cdot C_1^*(T)}{\int_0^T C_p^*(t) dt}. \quad \text{Eq. 2}$$

Normally  $k_4^*$  is not zero, resulting in a loss of FDG-6-PO<sub>4</sub> due to dephosphorylation. This loss of FDG-6-PO<sub>4</sub> at least partly compensates for the overestimation of MR caused by free FDG, adding further motivation for the use of Equation 2. What is still needed to calculate the MR is the integral in the denominator. This can be calculated by measuring the metabolic rate of glucose for erythrocytes. Assuming that the dephosphorylation in the erythrocytes is small, the accumulation of FDG-6-PO<sub>4</sub> in the erythrocytes is proportional to  $\int C_p^*(t) dt / C_{gl}$ . Their metabolism is very small, so most of the radioactivity in the cell is FDG and not FDG-6-PO<sub>4</sub>. Because FDG is an uncharged molecule, it diffuses freely through the membrane of the erythrocyte, in contrast to FDG-6-PO<sub>4</sub>, which is charged and is therefore trapped inside the erythrocyte. By washing the cells, researchers can remove the FDG leaving only FDG-6-PO<sub>4</sub>. To compensate for different metabolic rates of the erythrocytes, researchers determine this value by an in vitro incubation.

The metabolic rate for the erythrocytes in the bloodstream can then be written as:

$$MR_e = \frac{C_{gl}}{LCe} \frac{C_{M,e}^*(T)}{\int_0^T C_p^*(t) dt}. \quad \text{Eq. 3}$$

For the erythrocytes in the in vitro incubation, this can be expressed as:

$$MR_e = \frac{\bar{C}_{gl,i} C_{M,e,i}^*(T_i)}{LCe \bar{C}_{B,i}^* \cdot T_i}. \quad \text{Eq. 4}$$

The simple form of Equations 3 and 4 is because the free FDG has been removed by the washing procedure and dephosphorylation has been omitted. Combining Equations 3 and 4, we obtain:

$$\frac{\int_0^T C_p^*(t) dt}{C_{gl}} = \frac{\bar{C}_{B,i}^* \cdot C_{M,e}^*(T) \cdot T_i}{\bar{C}_{gl,i} \cdot C_{M,e,i}^*(T_i)}. \quad \text{Eq. 5}$$

The metabolic rate for tissue studied can then be expressed as:

$$MR = \frac{C_1^*(T) \cdot \bar{C}_{gl,i} \cdot C_{M,e,i}^*(T_i)}{\bar{C}_{B,i}^* \cdot C_{M,e}^*(T) \cdot T_i}. \quad \text{Eq. 6}$$

## MATERIALS AND METHODS

### Washing and Incubation Procedures

A venous blood sample of 8 ml, taken from the patient in the middle of the PET scan starting 45 min postinjection, is divided into three parts, which are treated as follows:

1. Approximately 1.5 ml of the blood sample is immediately transferred into a vial containing 50 ml of isotonic NaCl solution that contains 5 mmol/l of glucose. This has two purposes. First, it almost stops the FDG accumulation in blood cells, because the concentration of FDG is lowered by a factor of 30. Second, it is also part of the first washing process. With this dilution, a 1 hr delay before completing the analysis of the blood sample results in about a 6% higher value of FDG-6-PO<sub>4</sub> in the erythrocytes. To reduce the metabolism even further, the vial is stored at  $\sim 0^\circ\text{C}$ . The vial is then centrifuged at 1000 g for 5 min, after which all fluid is removed, leaving only the erythrocytes in the bottom of the vial. New NaCl solution (50 ml) described previously is added once more and the centrifugation is repeated. When the fluid has been removed again, samples from the fluid and the erythrocytes are taken for a radioactivity measurement. The radioactivity in the fluid is subtracted from the value of the erythrocytes sample to correct for remaining FDG activity. The correction is less than 5% of the value of the activity of the erythrocytes. The corrected activity in the erythrocytes is  $C_{M,e}^*(T)$ . In a control experiment with five washes, the activity measured in the erythrocytes after the first three washes was constant, thus indicating that no FDG-6-PO<sub>4</sub> is leaving the cells during the washing procedures.
2. 2.5 ml of the initial blood sample is used to determine the venous whole blood glucose level [ $C_{gl,i}(0)$ ]. As explained later, this value is only used in the incubation step 3.
3. To make a correction for individual variations of the erythrocyte glucose metabolism, an in vitro incubation must be performed. A volume of 4 ml of blood is injected into a vacutainer tub with about 200 kBq FDG ( $\sim 10 \mu\text{l}$ ) and is placed in a heating bath ( $37^\circ\text{C}$ ). The concentration of FDG in the vacutainer tub is 600 times higher than that in the bloodstream. This blood sample should incubate for approximately the same time as the delay from injection of FDG to the middle of the PET scan. The reason for this is that in vitro experiments have shown a nonlinear accumulation of FDG-6-PO<sub>4</sub> as a function of time, probably due to dephosphorylation. By keeping both time intervals approximately the same, the effect of dephosphorylation will be reduced. A small sample,  $\sim 0.5$  ml, is taken from the vacutainer tube at the end of the in vitro incubation to determine the radioactivity concentration ( $\bar{C}_{B,i}^*$ ). A 2-ml sample is taken to determine the venous whole blood glucose value [ $C_{gl,i}(T)$ ]. The rest of the blood sample, 1.5 ml, is transferred to a vial containing 50 ml of isotonic NaCl solution that contains 5 mmol/l of glucose. The blood sample from the in vitro incubation is handled in the same way as the blood sample 1. The radioactivity value determined for the erythrocytes from the in vitro incubation is  $C_{M,e,i}^*(T_i)$ . When the samples of the erythrocytes are taken, the topmost layer should not be used, because it can contain white blood cells with a much higher FDG-6-PO<sub>4</sub> concentration attention.

An automatic well-counter (7.62 cm  $\times$  7.62 cm NaI(Tl), 1282 Compugamma CS LKB/Wallac, Turku, Finland) was used to determine the radioactivity in all samples. Typical values for the different samples after administration of 74 MBq FDG and using 200 kBq FDG for the in vitro incubation can be seen in

**TABLE 1**  
Definitions of Symbols

Symbol	Definition
MR	Metabolic rate for glucose.
MR <sub>e</sub>	Metabolic rate for glucose in erythrocytes.
*	Asterisk denotes symbols that apply to FDG; symbols without asterisk apply to glucose.
C <sub>i</sub> <sup>*</sup> (T)	Tissue concentration of FDG plus FDG-6-PO <sub>4</sub> in a region I at a single time T.
C <sub>p</sub> <sup>*</sup> (t)	Input function; plasma concentration of FDG as a function of time (t).
k <sub>1</sub> <sup>*</sup> , k <sub>2</sub> <sup>*</sup>	Rate constants for FDG forward and reverse capillary membrane transport, respectively.
k <sub>3</sub> <sup>*</sup> , k <sub>4</sub> <sup>*</sup>	Rate constants for phosphorylation of FDG and dephosphorylation of FDG-6-PO <sub>4</sub> , respectively.
LC	Lumped constant.
LC <sub>e</sub>	Lumped constant for erythrocytes; because erythrocytes are in the plasma pool, LC <sub>e</sub> is only the ratio of phosphorylation for glucose and FDG.
C <sub>gl</sub>	Glucose concentration in the blood stream.
C <sub>gl,i</sub>	Mean value of β-glucose in the in vitro incubation, calculated from the β-glucose values at the beginning C <sub>gl,i</sub> (0) and at the end of incubation C <sub>gl,i</sub> (T <sub>i</sub> ).
C <sub>M,e</sub> <sup>*</sup> (T)	Concentration of FDG-6-PO <sub>4</sub> in erythrocytes in the blood stream at a single time T.
C <sub>M,e,i</sub> <sup>*</sup> (T <sub>i</sub> )	Concentration of FDG-6-PO <sub>4</sub> in erythrocytes after an in vitro incubation time of T <sub>i</sub> .
C <sub>B,i</sub> <sup>*</sup>	Mean value of concentration of FDG during the in vitro incubation, calculated as whole blood radioactivity minus 0.5 · C <sub>M,e,i</sub> <sup>*</sup> (T <sub>i</sub> ). The factor 0.5 is justified from the fact that all activity measurements are in the unit Bq/ml and that the hematocrit is close to 0.5, also 1 ml of blood contains white blood cells consuming the same amount of FDG as the erythrocytes. The value of 0.5 · C <sub>M,e,i</sub> <sup>*</sup> (T <sub>i</sub> ) is less than 2% of the whole blood activity, and this correction could be omitted.
T <sub>i</sub>	Time of in vitro incubation.

All radioactivity concentrations are corrected for decay.

Table 2. Due to the large difference in activity concentration, attention must be paid to reduce the risk of contamination from the in vitro incubation samples to the in vivo sample.

### Validation

The new method was validated in 16 patients. The value of the integrated input function estimated from the new method was compared to a calculated integrated input function from the same patient obtained from 24 blood samples. FDG was administered by a 2-min intravenous infusion into a peripheral vein in the arm. Arterial blood samples were not available, so venous blood samples for quantitative comparison were drawn from the other arm at every 20 sec for 4 min, every 1 min for 10 min and every 5 min up to a total time of 35 min. Blood glucose values were drawn from the same vein just before, 10 and 35 min after the injection of FDG. Using the results from Phelps et al. (1), the calculated integrated input function was increased by 5% to make it arterial-like. The blood sample for estimating the concentration of FDG-6-PO<sub>4</sub> in the erythrocytes was taken 35 min postinjection. The times for the in vitro incubations were, on average, 43 min for each patient. A quantitative comparison between the new method to estimate the integrated input function and the plasma activity integral divided by the glucose concentration was performed. The results are shown in Figure 1, with linear regression demonstrating

**TABLE 2**

Typical Values in the Different Samples After an Administration of 74 MBq FDG and Using 200 kBq FDG for the In Vitro Incubation

Samples	Count rate
C <sub>M,e</sub> <sup>*</sup> (T)	500 cpm for a 0.3-g sample
C <sub>M,e,i</sub> <sup>*</sup> (T <sub>i</sub> )	4500 cpm for a 0.2-g sample
C <sub>B,i</sub> <sup>*</sup>	80,000 cpm for a 0.2-g sample

The blood sample is taken 50 min postinjection.

excellent agreement between the two methods with a slope nearly equal to 1.0 (slope = 1.001, R<sup>2</sup> = 0.974).

### DISCUSSION

There are many routine clinical PET studies that use FDG, and they demand simple procedures for quantitative studies. In this article, we report on a new, simple method that provides an estimation of the integrated input function with an accuracy of better than ± 8%, using only one blood sample. One advantage of this method is that it measures the ratio between integrated FDG and glucose, meaning that minor fluctuations of the glucose level will not result in any errors in the metabolic rate for the tissue being studied. Also, the need of personnel during the uptake phase is eliminated, which furthermore reduces the absorbed dose to the technologist by 30 μSv per a typical 370 MBq FDG study. The handling of the samples with the new method takes about 15 min compared to 25 min for a conventional 24-sample study.

The validation is based on venous blood samples corrected by data from Phelps et al. (1). This correction, and the low sampling rate of glucose values, could contribute to the errors obtained with the new method. Due to the varying glucose consumption of the erythrocytes, an in vitro incubation must be performed for each study. This variation, up to 20%, is mainly caused by the age of the erythrocytes. Variation in age can be due to a variety of reasons, for example, bleeding (10). The glucose metabolism for erythrocytes is highly temperature dependent (11), ± 10% per degree change in temperature around 37°C. This means that the aforementioned equations are only valid for normo-thermic patients. Due to a dephosphorylation in the erythrocytes, it is important to keep the in vitro incubation time and the sampling time approximately equal. We have also used blood samples smaller than 2 ml, which is more difficult to handle. In this case, the glucose values are obtained

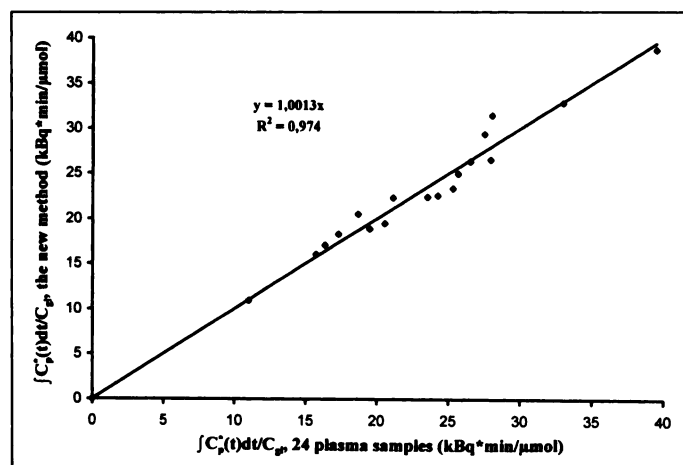


FIGURE 1. Correlation between the plasma activity integral divided by glucose concentration obtained from 24 venous plasma samples and the new method.

with a technique requiring only fractions of a milliliter. The rest of the samples are divided into two parts and are handled the same way as the larger samples described previously. This makes this method very practical for quantitative FDG studies on children, especially small children and newborns.

A semidynamic study based on two scan points, the first at 10–20 min and the second at 45–60 min postinjection, could be analyzed with the graphic method described by Patlak et al. (12), requiring only two blood samples that are treated as described previously. This simplified Patlak analysis will be validated in another study.

## CONCLUSION

A new method to normalize clinical routine FDG studies based on only one venous blood sample is presented. The method has been validated against a standard method with multiple blood samples showing an accuracy of better than  $\pm 8\%$ .

## ACKNOWLEDGMENTS

The authors thank Hans Lundqvist, PhD, Uppsala University and Mario Monti, Professor, University Hospital Lund, for helpful discussions. This work has been supported by grants from the Swedish Cancer Foundation grant 3320-B95-04XAB; the Gunnar, Arvid and Elisabeth Nilsson Foundation; the Mrs. Berta Kamprad Foundation; the John and Augusta Persson Foundation; the Royal Physiographic Society; the Lund Uni-

versity Medical Faculty; and the Lund University Hospital Fund.

## REFERENCES

1. Phelps ME, Huang SC, Hoffman EJ, et al. Tomographic measurement of local cerebral glucose metabolic rate in humans with (F-18)2-fluoro-2-deoxy-D-glucose: validation of method. *Ann Neurol* 1979;6:371–388.
2. Germano G, Chen BC, Huang S-C, Gambhir SS, Hoffman EJ, Phelps ME. Use of the abdominal aorta for arterial input function determination in hepatic and renal PET studies. *J Nucl Med* 1992;33:613–620.
3. Takikawa S, Dhawan V, Spetsieris P, et al. Noninvasive quantitative fluorodeoxyglucose PET studies with an estimated input function derived from a population-based arterial blood curve. *Radiology* 1993;188:131–136.
4. Lindholm P, Minn H, Leskinen-Kallio S, et al. Influence of the blood glucose concentration on FDG uptake in cancer—a PET study. *J Nucl Med* 1993;34:1–6.
5. Langen K-J, Braun U, Rota Kops E, et al. The influence of plasma glucose levels on fluorine-18-fluorodeoxyglucose uptake in bronchial carcinomas. *J Nucl Med* 1993;34:355–359.
6. Fischman AJ, Alpert NM. FDG-PET in oncology: there's more to it than looking at pictures. *J Nucl Med* 1993;34:6–11.
7. Chaiken L, Rege S, Hoh C, et al. Positron emission tomography with fluorodeoxyglucose to evaluate tumor response and control after radiation therapy. *Int J Radiat Oncol Biol Phys* 1993;27:455–464.
8. Brooks RA. Alternative formula for glucose utilization using labeled deoxyglucose. *J Nucl Med* 1982;23:538–539.
9. Rhodes CG, Wise RJS, Gibbs JM, et al. In vivo disturbance of the oxidative metabolism of glucose in human cerebral gliomas. *Ann Neurol* 1983;14:614–626.
10. Monti M, Wadsö I. Microcalorimetric measurements of heat production in human erythrocytes. IV. Comparison between different calorimetric techniques, suspension media, and preparation methods. *Scand J Clin Lab Invest* 1976;36:573–580.
11. Monti M, Wadsö I. Microcalorimetric measurements of heat production in human erythrocytes. III. Influence of pH, temperature, glucose concentration, and storage conditions. *Scand J Clin Lab Invest* 1976;36:565–572.
12. Patlak CS, Blasberg RG, Fenstermacher JD. Graphical evaluation of blood-to-brain transfer constants from multiple-time uptake data. *J Cereb Blood Flow Metab* 1983;3:1–7.

---

# Photon Energy Recovery: A Method to Improve the Effective Energy Resolution of Gamma Cameras

Pascal P. Hannequin and Jacky F. Mas

Centre d'Imagerie Nucléaire, Annecy; and Service de Médecine Nucléaire, Epinal, France

---

One of the major limitations of gamma cameras is their relatively poor energy resolution. The main practical consequence of this is that the detection of both scattered and unscattered photons in the photopeak energy window, affecting image contrast and resolution, makes the data inconsistent with the assumption of scatter-free projection data in reconstruction and attenuation correction algorithms. Here, we proposed a method to improve the effective energy resolution of scintigraphic acquisitions. This method is called photon energy recovery (PER). **Methods:** Photon energy recovery is based on a spectral deconvolution analysis and uses iterative recurrent linear regressions. In practice, PER only required splitting the photopeak energy window into several subwindows and did not need list mode acquisitions. The method was fully automated. Photon energy recovery was quantitatively validated on  $^{99m}\text{Tc}$  planar images using a Monte Carlo simulation and a real phantom and was illustrated by a bone study. **Results:** The Monte Carlo simulation demonstrated that convergence was reached within relatively few (10–15) iterations. Photon energy recovery led to a considerable quantitative improvement because the mean error between the photopeak energy window image and the true unscattered image was equal to 8.72 s.d. (the mean error between one image and the true image was the mean of the differences between the two

images; the difference is expressed as several s.d., where s.d. was the square root of the true value), whereas the mean error between the 140-keV PER image and the true unscattered image was only equal to 2.70. Moreover, the true and PER spectra were highly correlated. The real phantom data pointed out that the counts in the 140-keV PER image calculated from the images acquired “with scatter” were not very different from the true counts given by the “scatter-free” reference image. Planar pelvic bone scintigraphy demonstrated the advantages of PER because contrast increased when only unscattered photons were selected. **Conclusion:** Photon energy recovery is a stable and automated method that allows recovery of the correct value of the photon energy after a scintigraphic acquisition. Its ability to separate scattered from unscattered events has been quantitatively validated.

**Key Words:** scatter correction; spectral deconvolution; SPECT

**J Nucl Med** 1996; 39:555–562

---

One of the major limitations of gamma cameras is their relatively poor energy resolution. In fact, the spectral response of the detector is not a Dirac distribution but a Gaussian one. At 140 keV, the gamma energy of  $^{99m}\text{Tc}$ , the energy resolution is slightly less than 10% on modern gamma cameras. This imposes the use of relatively wide photopeak energy windows to collect most of the photons of interest, that is, the primary

Received Nov. 21, 1996; revision accepted May 8, 1997.

For correspondence or reprints contact: Pascal P. Hannequin, MD, PhD, Centre d'Imagerie Nucléaire, 4, Chemin de la Tour de la Reine, 74000 Annecy, France.